Journal of AI and Data Mining
Vol 4, No 1, 2016, 93-102 ***10.5829/idosi.JAIDM.2016.04.01.11***

Trajectory tracking of under-actuated nonlinear dynamic robots: Adaptive fuzzy hierarchical terminal sliding-mode control

Y. Vaghei and A. Farshidianfar*

Mechanical Engineering Department, Ferdowsi University of Mashhad, Mashhad, Iran.

Received 21 April 2015; Accepted 28 November 2015
**Corresponding author: farshid@um.ac.ir (A. Farshidianfar).*

Abstract Under-actuated nonlinear dynamic systems trajectory tracking, such as space robots and manipulators with structural flexibility, has recently been investigated for hierarchical sliding mode control since these systems require complex computations. However, the instability phenomena possibly occur especially for long-term operations. In this paper, a new design approach of an adaptive fuzzy hierarchical terminal sliding-mode controller (AFHTSMC) is proposed. The sliding surfaces of the subsystems construct the hierarchical structure of the proposed method in which the top layer includes all of the subsystems' sliding surfaces. Moreover, a terminal-sliding mode has been implemented in each layer to ensure the error convergence to zero in finite time besides chattering reduction. In addition, online fuzzy models are employed to approximate the two nonlinear dynamic system's functions. Finally, a simulation example of an inverted pendulum is proposed to confirm the effectiveness and robustness of the proposed controller.

Keywords: *Adaptive Fuzzy System, Hierarchical Structure, Terminal Sliding Mode Control, Under-actuated System.*

1. Introduction

In the recent years, interests toward developing under-actuated systems have been increased. Many of mechanical systems often have the under-actuation problem in which the system is not able to follow arbitrary trajectories in configuration space. This occurs if the system has a lower number of actuators than its degrees of freedom. In this condition, the system is said to be trivially under-actuated. These systems cover a wide range of applications in our everyday lives such as overhead cranes, space robots, automobiles with non-holonomic constraints, and legged robots [1-3].

Many researchers investigated the control of under-actuated systems. In this paper, the focus is on variable structure systems (VSS) due to their effective control scheme in dealing with uncertainties, noise, and time varying properties [4,5]. One of the robust design methodologies of VSS is the sliding mode control chooses switching manifolds, which are usually linear hyper-planes that guarantee the asymptotic stability shown by the Lyapunov's stability theorem [6,7]. In high precision applications, fast convergence may not be delivered without strict control. Hence, in order to overcome this problem, a terminal sliding mode (TSM) control has recently been developed. It enables the fast finite time convergence and ensures less steady state errors. However, the existence of the singularity problem in the conventional TSM controller design methods is a common drawback [8,9]. Several methods have been proposed to solve this problem.

The TSM control methods can be divided into two approaches: the indirect approach and the direct approach, in which the controllers require discontinuous control leading to undesirable chattering. In an indirect approach [10], scientists implemented switching from terminal sliding manifold to linear sliding manifold in order to avoid the singularity problem. In addition, some efforts have been made to transfer the trajectory to a specified open non-singular region [11]. Also, a direct approach has been investigated for a class of nonlinear dynamical systems with parameter uncertainties and external disturbances in [12]. Later, fuzzy TSM controllers [13] were

introduced to solve the problems caused by these two approaches and under-actuated systems with unknown nonlinear system functions [14,18]. In addition, there has been growing attention paid to the adaptive fuzzy TSM in various control problems [19].

In further studies, efforts have been made to overcome the problems of the fuzzy sliding mode control and fuzzy TSM control. Hierarchical structures shown their effectiveness according to their ability to achieve the ideal decoupling performance with guaranteed stability [20]. The implementation of these structures enables us to decouple a class of nonlinear coupled systems into several subsystems. Also, the sliding surfaces, which govern the states' responses, are defined for each subsystem. In these systems, first, a sliding surface is defined for each subsystem. Then, the first-layer sliding surface constructs the second-layer sliding surface. This process continues to achieve the last sliding mode surface (hierarchical surface). In literature, the Lyapunov theorem has been employed to prove the stability of the closed-loop system for the single-input system. There are a few studies on the effectiveness of the adaptive fuzzy law derivation for the coupling factor tuning [21-23]; however, the chattering and fast convergence problems are still remained unsolved.

As can be clearly seen in the aforementioned studies, the implementation of the adaptive fuzzy system besides the sliding mode and hierarchical structure could not solve the chattering and fast time convergence problems; therefore, in this study, our main objective is to propose a novel control method, named as the adaptive fuzzy hierarchical terminal sliding mode control (AFHTSMC), which enables us to use the advantages of terminal sliding mode control besides the adaptive fuzzy hierarchical structure for uncertain under-actuated nonlinear dynamic systems control. The main features of the proposed AFHTSMC are as follows: 1) The implementation of the TSM control, which guarantees the fast finite time convergence and reduces the chattering and steady state errors. This superior property becomes admirable in the applications requiring high precision; 2) The unknown nonlinear system functions are approximated by the adaptive fuzzy systems with adaptive learning laws; 3) The hierarchical structure of the proposed method is also a very effective tool to guarantee the stability, especially for complex and high nonlinear dynamic systems.

In Section II, the system's description and the control objectives are presented. Then AFHTSMC development for dealing with the trajectory tracking control problem of uncertain under-actuated nonlinear dynamic systems is introduced in Section III. Section IV is dedicated to the Lyapunov stability analysis of the proposed closed-loop system. The simulations, results and discussions are presented in Section V for an inverted pendulum on a cart. Finally, concluding remarks are made in Section VI.

2. System description and problem formulation

An under-actuated single-input-multi-output system with uncertainty and nonlinear coefficients is defined in (1).

$$\begin{cases} \dot{x}_1(t) = x_2(t) \\ \dot{x}_2(t) = f_1(x) + b_1(x)\,u(t) + d_1(x,t) \\ \dot{x}_3(t) = x_4(t) \\ \dot{x}_4(t) = f_2(x) + b_2(x)\,u(t) + d_2(x,t) \\ \quad\vdots \\ \dot{x}_{2n-1}(t) = x_{2n}(t) \\ \dot{x}_{2n}(t) = f_n(x) + b_n(x)\,u(t) + d_n(x,t) \end{cases} \tag{1a}$$

$$y(t) = [x_1(t)\; x_3(t) \ldots x_{2n-1}(t)]^T \tag{1b}$$

where, $x(t) = [x_1(t)\; x_2(t) \ldots x_{2n}(t)]^T \in \Re^{2n}$ is the system state variable, $f_i(x)$ and $b_i(x)$, i=1,2, …, n are unknown nominal nonlinear functions, $(0 \le d_i(x,t) \le \rho_i,\ i=1,2,\ \ldots,\ n)$ are bounded time-varying disturbances, and $u(t)$ and $y(t)$ are the control input and the system output, respectively. The contribution of this paper is to design the hierarchical terminal sliding mode controller with adaptive fuzzy learning laws for a class of uncertain under-actuated nonlinear dynamic systems (UUND). Figure 1 shows that the adaptive learning laws are applied to adjust the parameter vectors of fuzzy systems for approximation of uncertain nonlinear system functions.

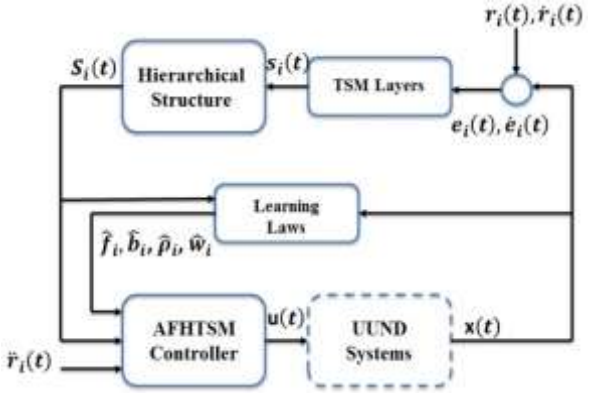

Figure 1. The schematic overall control block-diagram.

Also, the performance of the bounded trajectory tracking and asymptotical trajectory tracking are addressed. Finally, the simulation results of an inverted pendulum on a movable cart with bounded external disturbance are investigated.

3. AFHTSMC development

3.1. The terminal sliding surfaces

In this section, initially, the conventional terminal sliding surfaces are defined in (2-4).

$$s_i(t) = \dot{e}_i(t)^{\gamma_i} + c_i e_i(t) \quad (2)$$

where, for i=1,2,…,n, the reference inputs are $r_i(t)$, c_i and $\gamma_i = \frac{p}{q}$ are positive constants, and p and q are odd positive integers.

$$e_i(t) = x_{2i-1}(t) - r_i(t) \quad (3)$$

$$\dot{e}_i(t) = x_{2i}(t) - \dot{r}_i(t) \quad (4)$$

However, the singularity problem may occur in this structure because of the term $c_i \frac{q}{p} e_i^{\frac{q-p}{p}}(t)\dot{e}_i(t)$ in the control input. If the $2q > p > q$ is chosen, the term $e_i^{\frac{q-p}{p}}(t)$ will be equal to $e_i^{\frac{2q-p}{p}}(t)$ which will be nonsingular. On the other hand, if little control to enforce $e_i(t) \neq 0$ is made while $\dot{e}_i(t) \neq 0$, the singularity problem occurs. Hence, an indirect approach has been implemented to avoid this problem and define the terminal sliding surfaces in (5).

$$s_i(t) = \dot{e}_i(t)^{\gamma_i} + c_i e_i(t) \quad (5)$$

It has to be noticed that the derivative of $s_i(t)$ along the system's dynamics does not result in terms with negative (fractional) powers by using (5) and the singularity is avoided by switching between (2) and (5), where the error and its derivative are bounded as in [20]. In this problem, designing a switched control that drives the plant state to the switching surface and maintain it on the surface upon interception is the most important achievement. As can be seen, the system motion is governed by c_i, which is an integer number. This number's value indicates the effect of error on the sliding surface and it is selected based on the $\dot{e}_i(t)^{\gamma_i}$ value, while $s_i(t)$ in each layer has a crucial effect on the system's control. It is important to mention that high values of c_i increase the effect of e_i in each layer and may result in misleading the controller; hence, appropriate values of c_i are required to maintain a high precision control system. Further studies can be found in section 3.2.

3.2. The hierarchical structure

In the next step, after the definition of the sliding surfaces, higher hierarchical levels $(S_i(t))$ are created by lower TSM surfaces $(s_i(t))$ as shown in figure 2. The i^{th} hierarchical layer sliding surface is defined in (6).

$$S_i(t) = \lambda_{i-1} S_{i-1}(t) + s_i(t) \quad (6)$$

where, λ_{i-1} is constant when $\lambda_0 = S_0 = 0$. The value of the λ_{i-1} parameter indicates the effectiveness of the last hierarchical layers in comparison with the current sliding surface. Larger values of λ_{i-1} increase the value amount that is given to the prior layers instead of the highest hierarchical sliding surface. This parameter has to be adjusted so as to satisfy the Lyapunov theorem and the required accuracy.

Furthermore, the control input for the i^{th} layer $u_i(t)$ consists of the equivalent and the switching control terms besides the last control input $u_{i-1}(t)$, which is shown in (7).

$$u_i(t) = u_{i-1}(t) + \hat{u}_{eq,i}(t) + \hat{u}_{sw,i}(t) \quad (7)$$

where, $u_0 = 0$ and

$$\hat{u}_{eq,i}(t) = -\frac{\left[\hat{f}_i(x|\hat{\theta}_{f_i}) - \ddot{r}_i(t) + c_i\gamma_i{}^{-1}\dot{e}_i^{2-\gamma_i} + ksgn(s_i)\right]}{\hat{b}_i(x|\hat{\theta}_{b_i})} \quad (8)$$

$$\hat{u}_{sw,i}(t) = -\sum_{1}^{i-1}\hat{u}_{sw,l}(t) - \frac{\left\{\sum_{l=1}^{i}[\sum_{\substack{m=1\\m\neq l}}^{i}(\prod_{j=m}^{i} a_j)\hat{b}_m(x|\hat{\theta}_{b_m})]\right\} \times \hat{u}_{eq,l}(t) + k_i S_i(t) + sgn(S_i)\hat{\omega}(t)}{\sum_{m=1}^{i}(\prod_{j=m}^{i} a_j)\hat{b}_m(x|\hat{\theta}_{b_m})} \quad (9)$$

where, $\hat{f}_i$, $\hat{b}_i$ are the approximations of the unknown nonlinear functions. $f_i(x)$ and $b_i(x)$ are defined in (13,14). $\ddot{r}_i(t)$ is the second derivative of reference input , $a_j = \lambda_j$ as $j \neq i$ and $a_j = 1$ as $j = i$, i=1,2,…,n.

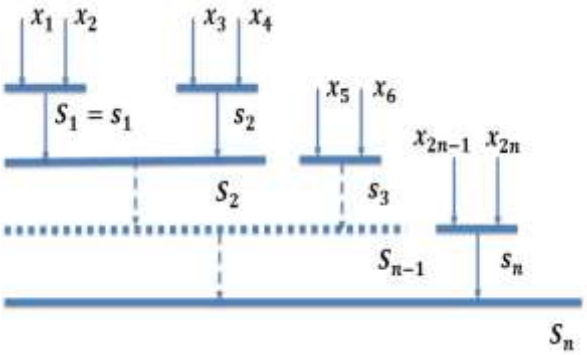

Figure 2. The hierarchical TSM layers construction.

3.3. Adaptive fuzzy inference system

In order to improve the system effectiveness, the unknown uncertain continuous nonlinear functions, $f_i(x), b_i(x)$ and $\rho_i(x)$ are to be learned by the learning functions. The fuzzy rule base is defined in (10).

$$R^{(l)}: \text{IF } x_1 \text{ is } F_1^l \text{ and } \dots \text{ and } x_{2n} \text{ is } F_{2n}^l, \quad \text{THEN y is } G^l \tag{10}$$

where, F_i^l and G_i^l are the input and the output of the fuzzy systems, respectively. The crisp point x is mapped from fuzzy sets U to a crisp point V, based on the fuzzy IF-THEN rules and by means of the fuzzifier and defuzzifier. The output of the fuzzy system is shown in (11), based on singleton fuzzifier, center-average deffuzification, and product inference engine.

$$y = \theta^T \xi(x) \tag{11}$$

in which, $\theta^T = [\theta^T\ \theta^T \dots \theta^T] \in \Re^M$ are the points that have the maximum value of membership functions that G^l is able to achieve and $\xi(x) = [\xi^1(x)\ \xi^2(x) \dots \xi^M(x)]^T$ are basis functions defined as in (12).

$$\xi^l(x) = \frac{\prod_{i=1}^{2n} \mu_{F_i^l}(x_i)}{\sum_{l=1}^{M} \prod_{i=1}^{2n} \mu_{F_i^l}(x_i)} \tag{12}$$

where, $\mu_{F_i^l}(x_i)$ is the membership function of the fuzzy set. The approximation of the unknown nonlinear functions $f_i(x), b_i(x)$ and $\rho_i(x)$ are defined as in (13-15).

$$\hat{f}_i(x|\hat{\theta}_{f_i}) = \hat{\theta}_{f_i}^T \xi(x) \tag{13}$$

$$\hat{b}_i(x|\hat{\theta}_{b_i}) = \hat{\theta}_{b_i}^T \xi(x) \tag{14}$$

$$\hat{\rho}_i(x|\hat{\theta}_{\rho_i}) = \hat{\theta}_{\rho_i}^T \xi(x) \tag{15}$$

Also, the optimal parameters will be defined in (16-18).

$$\theta_{f_i}^* = \arg_{\hat{\theta}_{f_i}(t)\in\Omega_{\hat{\theta}_{f_i}}} \min \sup_{x(t)\in\Omega_x} \{|\hat{f}_i(x|\hat{\theta}_{f_i}) - f_i(x)|\} \tag{16}$$

$$\theta_{b_i}^* = \arg_{\hat{\theta}_{f_i}(t)\in\Omega_{\hat{\theta}_{b_i}}} \min \sup_{x(t)\in\Omega_x} \{|\hat{b}_i(x|\hat{\theta}_{b_i}) - b_i(x)|\} \tag{17}$$

$$\theta_{\rho_i}^* = \arg_{\hat{\theta}_{\rho_i}(t)\in\Omega_{\hat{\theta}_{\rho_i}}} \min \sup_{x(t)\in\Omega_x} \{|\hat{\rho}_i(x|\hat{\theta}_{\rho_i}) - \rho_i(x)|\} \tag{18}$$

And the learning laws of parameter vectors are designed as in [19, 20].

In addition, the upper bound of uncertainties is defined in (19).

$$\dot{\tilde{\omega}} = \begin{cases} \gamma_w |S_i(t)| & \text{if } |\tilde{\omega}| < N_w \\ \gamma_w |S_i(t)| - \delta_w |S_i(t)| \tilde{\omega}(t) & \text{if } |\tilde{\omega}| \geq N_w \end{cases} \tag{19}$$

where, $\gamma_w > 0$ is the learning gain and $\delta_w > 0$ is the projection gain.

Hence, (20, 21) are obtained for AFHTSMC.

$$S_n(t) = \sum_{m=1}^{n} \left(\prod_{j=m}^{i} a_j \right) s_m(t) \tag{20}$$

$$u_n(t) = \sum_{l=1}^{n} \hat{u}_{sw,l}(t) + \hat{u}_{eq,l}(t) \tag{21}$$

4. Stability analysis

The following Lyapunov functions are considered in order to prove the stability of the proposed control method. Here, it has been assumed that the learning parameters are bounded and no projection term is required for the learning laws.

$$V_i = \left\{ S_i^2 + \sum_{m=1}^{i} \left[\frac{\tilde{\theta}_{f_m}^T \tilde{\theta}_{f_m}}{\gamma_{f_m}} + \frac{\tilde{\theta}_{b_m}^T \tilde{\theta}_{b_m}}{\gamma_{b_m}} + \frac{\tilde{\theta}_{\rho_m}^T \tilde{\theta}_{\rho_m}}{\gamma_{\rho_m}} \right] + \tilde{\omega}^2/\gamma_\omega \right\} /2 \tag{22}$$

$$\dot{V}_i = S_i \dot{S}_i + \frac{\tilde{\omega}\dot{\tilde{\omega}}}{\gamma_\omega} + \sum_{m=1}^{i} \left[\frac{\tilde{\theta}_{f_m}^T \dot{\tilde{\theta}}_{f_m}}{\gamma_{f_m}} + \frac{\tilde{\theta}_{b_m}^T \dot{\tilde{\theta}}_{b_m}}{\gamma_{b_m}} + \frac{\tilde{\theta}_{\rho_m}^T \dot{\tilde{\theta}}_{\rho_m}}{\gamma_{\rho_m}} \right] \tag{23}$$

$$\dot{V}_i = S_i \sum_{m=1}^{n} \left(\prod_{j=m}^{i} a_j \right) \dot{s}_m(t) + \frac{\tilde{\omega}\dot{\tilde{\omega}}}{\gamma_\omega} + \sum_{m=1}^{i} \left[\frac{\tilde{\theta}_{f_m}^T \dot{\tilde{\theta}}_{f_m}}{\gamma_{f_m}} + \frac{\tilde{\theta}_{b_m}^T \dot{\tilde{\theta}}_{b_m}}{\gamma_{b_m}} + \frac{\tilde{\theta}_{\rho_m}^T \dot{\tilde{\theta}}_{\rho_m}}{\gamma_{\rho_m}} \right] \tag{24}$$

$$= S_i \sum_{m=1}^{n} \left(\prod_{j=m}^{i} a_j \right) [c_m \dot{e}_m + \gamma_m \dot{e}_m{}^{\gamma_m - 1} (f_m + b_m u + d_m - \ddot{r}_m) + \frac{\tilde{\omega}\dot{\tilde{\omega}}}{\gamma_\omega} + \sum_{m=1}^{i} \left[\frac{\tilde{\theta}_{f_m}^T \dot{\tilde{\theta}}_{f_m}}{\gamma_{f_m}} + \frac{\tilde{\theta}_{b_m}^T \dot{\tilde{\theta}}_{b_m}}{\gamma_{b_m}} + \frac{\tilde{\theta}_{\rho_m}^T \dot{\tilde{\theta}}_{\rho_m}}{\gamma_{\rho_m}} \right] \tag{25}$$

$$\leq S_i \sum_{m=1}^{n} \left(\prod_{j=m}^{i} a_j \right) [c_m \dot{e}_m + \gamma_m \dot{e}_m{}^{\gamma_m - 1} (f_m + b_m u - \ddot{r}_m) + |S_i| \sum_{m=1}^{i} \left| \left(\prod_{j=m}^{i} a_j \right) \right| \gamma_m \dot{e}_m{}^{\gamma_m - 1} \rho_m + \frac{\tilde{\omega}\dot{\tilde{\omega}}}{\gamma_\omega} + \sum_{m=1}^{i} \left[\frac{\tilde{\theta}_{f_m}^T \dot{\tilde{\theta}}_{f_m}}{\gamma_{f_m}} + \frac{\tilde{\theta}_{b_m}^T \dot{\tilde{\theta}}_{b_m}}{\gamma_{b_m}} + \frac{\tilde{\theta}_{\rho_m}^T \dot{\tilde{\theta}}_{\rho_m}}{\gamma_{\rho_m}} \right] \tag{26}$$

$$= S_i \sum_{m=1}^{n} \left(\prod_{j=m}^{i} a_j \right) [c_m \dot{e}_m + \gamma_m \dot{e}_m{}^{\gamma_m - 1} ([f_m - \hat{f}_m^*] + [\hat{f}_m^* - \hat{f}_m] + \hat{f}_m + [b_m u - \hat{b}_m^* u] + [b_m^* u - \hat{b}_m u] + b_m u - \ddot{r}_m) + |S_i| \sum_{m=1}^{i} \left| \left(\prod_{j=m}^{i} a_j \right) \right| \gamma_m \dot{e}_m{}^{\gamma_m - 1} \{ [\rho_m - \hat{\rho}_m^*] + [\hat{\rho}_m^* - \hat{\rho}_m] + \hat{\rho}_m \} + \frac{\tilde{\omega}\dot{\tilde{\omega}}}{\gamma_\omega} + \sum_{m=1}^{i} \left[\frac{\tilde{\theta}_{f_m}^T \dot{\tilde{\theta}}_{f_m}}{\gamma_{f_m}} + \frac{\tilde{\theta}_{b_m}^T \dot{\tilde{\theta}}_{b_m}}{\gamma_{b_m}} + \frac{\tilde{\theta}_{\rho_m}^T \dot{\tilde{\theta}}_{\rho_m}}{\gamma_{\rho_m}} \right] \quad (27)$$

$$\leq S_i \omega + S_i \sum_{m=1}^{n} \left(\prod_{j=m}^{i} a_j \right) [c_m \dot{e}_m + \gamma_m \dot{e}_m{}^{\gamma_m - 1} ([\hat{f}_m^* - \hat{f}_m] + \hat{f}_m + [b_m^* u - \hat{b}_m u] + b_m u - \ddot{r}_m) + |S_i| \sum_{m=1}^{i} \left| \left(\prod_{j=m}^{i} a_j \right) \right| \gamma_m \dot{e}_m{}^{\gamma_m - 1} \{ [\hat{\rho}_m^* - \hat{\rho}_m] + \hat{\rho}_m \} + \frac{\tilde{\omega}\dot{\tilde{\omega}}}{\gamma_\omega} + \sum_{m=1}^{i} \left[\frac{\tilde{\theta}_{f_m}^T \dot{\tilde{\theta}}_{f_m}}{\gamma_{f_m}} + \frac{\tilde{\theta}_{b_m}^T \dot{\tilde{\theta}}_{b_m}}{\gamma_{b_m}} + \frac{\tilde{\theta}_{\rho_m}^T \dot{\tilde{\theta}}_{\rho_m}}{\gamma_{\rho_m}} \right] \quad (28)$$

$$= S_i \omega + S_i \sum_{m=1}^{n} \left(\prod_{j=m}^{i} a_j \right) [c_m \dot{e}_m + \gamma_m \dot{e}_m{}^{\gamma_m - 1} \left([\theta_{f_m}^{*T} \xi - \hat{\theta}_{f_m}{}^T \xi] + \hat{f}_m + [\theta_{b_m}^{*T} \xi - \hat{\theta}_{b_m}{}^T \xi] + b_m u - \ddot{r}_m \right) + |S_i| \sum_{m=1}^{i} \left| \left(\prod_{j=m}^{i} a_j \right) \right| \gamma_m \dot{e}_m{}^{\gamma_m - 1} \{ [\theta_{\rho_m}^{*T} \xi - \hat{\theta}_{\rho_m}{}^T \xi] + \hat{\rho}_m \} + \frac{\tilde{\omega}\dot{\tilde{\omega}}}{\gamma_\omega} + \sum_{m=1}^{i} \left[\frac{\tilde{\theta}_{f_m}^T \dot{\tilde{\theta}}_{f_m}}{\gamma_{f_m}} + \frac{\tilde{\theta}_{b_m}^T \dot{\tilde{\theta}}_{b_m}}{\gamma_{b_m}} + \frac{\tilde{\theta}_{\rho_m}^T \dot{\tilde{\theta}}_{\rho_m}}{\gamma_{\rho_m}} \right] \quad (29)$$

$$= S_i \omega + S_i \sum_{m=1}^{n} \left(\prod_{j=m}^{i} a_j \right) [c_m \dot{e}_m + \gamma_m \dot{e}_m{}^{\gamma_m - 1} (\hat{f}_m + b_m u - \ddot{r}_m) + |S_i| \sum_{m=1}^{i} \left| \left(\prod_{j=m}^{i} a_j \right) \right| \gamma_m \dot{e}_m{}^{\gamma_m - 1} \{ \hat{\rho}_m \} + \frac{\tilde{\omega}\dot{\tilde{\omega}}}{\gamma_\omega} - S_i \sum_{m=1}^{i} \left(\prod_{j=m}^{i} a_j \right) \tilde{\theta}_{f_m}^T \xi + \sum_{m=1}^{i} \tilde{\theta}_{f_m}^T \hat{\theta}_{f_m}^T / \gamma_{f_m} - S_i \sum_{m=1}^{i} \left(\prod_{j=m}^{i} a_j \right) \tilde{\theta}_{b_m}^T \xi u + \sum_{m=1}^{i} \tilde{\theta}_{b_m}^T \hat{\theta}_{b_m}^T / \gamma_{b_m} - |S_i \sum_{m=1}^{i} \left(\prod_{j=m}^{i} a_j \right) | \tilde{\theta}_{\rho_m}^T \xi + \sum_{m=1}^{i} \tilde{\theta}_{\rho_m}^T \hat{\theta}_{\rho_m}^T / \gamma_{f_m} \quad (30)$$

Hence, we replace the terms $\hat{f}_m^*, \hat{f}_m, b_m^*$ and $\hat{b}_m$ by $\theta_{f_m}^{*T} \xi$, $\hat{\theta}_{f_m}{}^T \xi$, $\theta_{b_m}^{*T} \xi$ and $\hat{\theta}_{b_m}{}^T \xi$, respectively. This leads to (29) and discretization gives (30). Substituting the learning laws and the control law of the i^{th}layer and the learning upper bound of uncertainties into the above equation yields (31-35).

$$= |S_i| \omega + \frac{\tilde{\omega}\dot{\tilde{\omega}}}{\gamma_\omega} + S_i \sum_{m=1}^{n} \left(\prod_{j=m}^{i} a_j \right) [c_m \dot{e}_m + \gamma_m \dot{e}_m{}^{\gamma_m - 1} \left(f_m + b_m \hat{u}_{eq,m} + b_m \left(\sum_{\substack{l=1 \\ l \neq m}}^{i} \hat{u}_{eq,l} + \sum_{l=1}^{i} \hat{u}_{sw,l} \right) - \ddot{r}_m \right)] + |S_i| \sum_{m=1}^{i} \left| \left(\prod_{j=m}^{i} a_j \right) \right| \gamma_m \dot{e}_m{}^{\gamma_m - 1} \rho_m \quad (31)$$

$$= |S_i| \omega + \frac{\tilde{\omega}\dot{\tilde{\omega}}}{\gamma_\omega} + S_i \sum_{m=1}^{n} \left(\prod_{j=m}^{i} a_j \right) [c_m \dot{e}_m + \gamma_m \dot{e}_m{}^{\gamma_m - 1} \left(f_m + b_m \sum_{l=1}^{i} \hat{u}_{sw,l} + \hat{u}_{eq,l} - \ddot{r}_m \right)] + |S_i| \sum_{m=1}^{i} \left| \left(\prod_{j=m}^{i} a_j \right) \right| \gamma_m \dot{e}_m{}^{\gamma_m - 1} \rho_m \quad (32)$$

$$= |S_i| \omega + \frac{\tilde{\omega}\dot{\tilde{\omega}}}{\gamma_\omega} + S_i \sum_{m=1}^{n} \left(\prod_{j=m}^{i} a_j \right) [\gamma_m \dot{e}_m{}^{\gamma_m - 1} \left(b_m \left(\sum_{\substack{l=1 \\ l \neq m}}^{i} \hat{u}_{eq,l} + \sum_{l=1}^{i} \hat{u}_{sw,l} \right) \right)] + |S_i| \sum_{m=1}^{i} \left| \left(\prod_{j=m}^{i} a_j \right) \right| \gamma_m \dot{e}_m{}^{\gamma_m - 1} \rho_m \quad (33)$$

$$\leq |S_i| \omega + \frac{\tilde{\omega}\dot{\tilde{\omega}}}{\gamma_\omega} - K |S_i| \dot{e}_m{}^{\gamma_m - 1} \omega \quad (34)$$

$$\leq -K_1 S_i^2 - K |S_i| \dot{e}_m{}^{\gamma_m - 1} \omega < 0 \quad (35)$$

5. Simulations and discussions

The inverted pendulum on a movable cart is considered to verify the effectiveness of the proposed controller (Figure 3). Here, the system functions are described in (36-39).

$$f_1(x) = \frac{\{m_t g \sin x_1 - m_p L \sin x_1 \cos x_1 x_2^2\}}{L/2 \left(\frac{4m_t}{3} - m_p \cos^2 x_1 \right)} \quad (36)$$

$$f_2(x) = \frac{\left\{ -\frac{4m_p L}{2} x_2^2 \sin \frac{x_1}{3} + m_p g \sin x_1 \cos x_1 \right\}}{\left(\frac{4m_t}{3} - m_p \cos^2 x_1 \right)} \quad (37)$$

$$b_1(x) = \cos\frac{x_1}{\frac{L}{2}\left(\frac{4m_t}{3} - m_p\cos^2 x_1\right)} \quad (38)$$

$$b_2(x) = \frac{4}{3\left(\frac{4m_t}{3} - m_p\cos^2 x_1\right)} \quad (39)$$

where, $m_t = m_p + m_c$ and x_1 , x_2 , x_3 , x_4 are respectively the pendulum's angle with respect to the vertical axis, the angular velocity of the pendulum with respect to the vertical axis, the position of the cart, and the velocity of the cart. The magnitudes of the constant parameters of the system are shown in table 1.

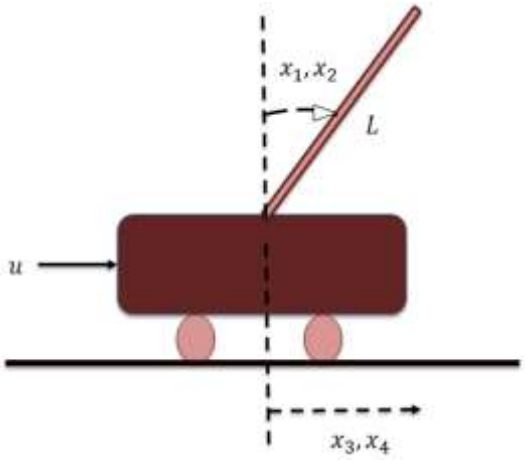

Figure 3. The inverted pendulum on a movable cart.

The simulations have been done by MATLAB 2012 software. Since the term x_i is used in the Lyapunov function and adaptation laws, it has to be fuzzified in order to achieve the results for the output of the system. Hence, x_i is input variable of the fuzzy system and u is its output variable, respectively. The membership functions are assumed to be triangular because they result in entropy equalization in probability density function.

Table 1. The constant parameter's magnitudes of the system.

Parameter	Magnitude	Description
m_c	1 Kg	Mass of the cart
m_p	0.05 Kg	Mass of the pendulum
L	1 m	Length of the pendulum
g	9.806 $\frac{m}{s^2}$	Acceleration due to gravity

Also, the reconstruction will be error-free if a ½ overlap between neighbouring fuzzy sets is considered. When interfacing fuzzy sets are being constructed by numerical datum, these two characteristics are implemented. Based on the aforementioned reasons, the membership functions are designed as shown in figures 4 and 5.

As can be clearly seen, each of the inputs and the outputs are partitioned by seven membership functions called as negative big (NB), negative medium (NM), negative small (NS), zero (Z), positive small (PS), positive medium (PM), and positive big (PB). Of course, one can alter the membership functions type and number in order to improve the results.

In this research, the reference inputs are set as $r_1(t) = 5.5\sin(t)$ (degree) and $r_2(t) = \sin(t)$ (m). The hierarchical terminal sliding surfaces are selected as $s_1(t) = \dot{e}_1(t)^{\gamma_1} + c_1 e_1(t)$ and $s_2(t) = \dot{e}_2(t)^{\gamma_1} + c_2 e_2(t)$ where $c_1 = 2$, $c_2 = 1$ and $\gamma_1 = \gamma_2 = \frac{9}{7}$. The initial values are chosen as $x(0) = [\frac{\pi}{6}, 0, 0, 0]$. In addition, we assume the external disturbance to be a low frequency signal, $d_1(x,t) = 0.75x_1^2(t)\sin(\sin(t)\,x_1x_3)$, and a high frequency signal, $d_2(x,t) = 0.75x_3x_4\sin(100(t))$.

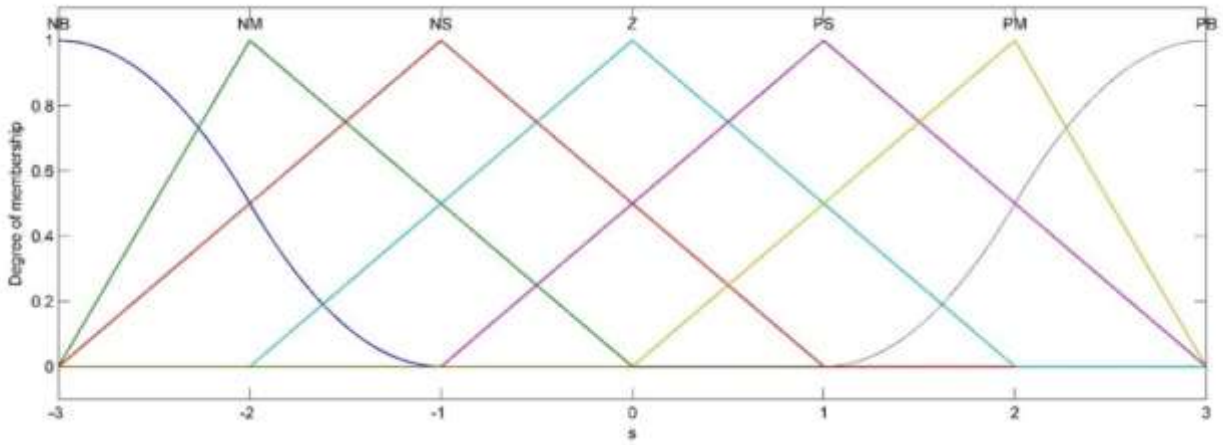

Figure 4. The membership functions of the input variables.

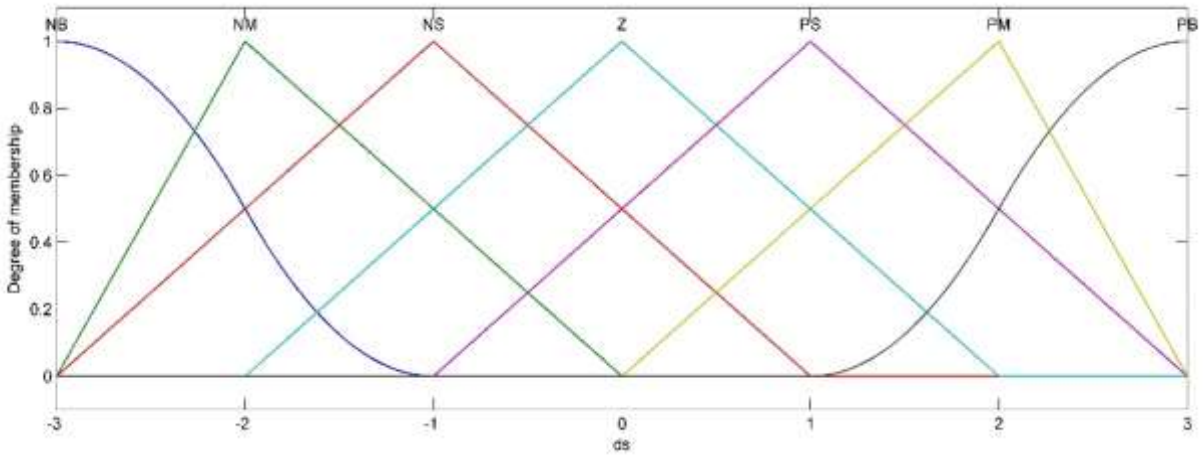

Figure 5. The membership functions of the output variable.

In order to verify the reliability of the proposed AFHTSMC, long-term operation simulations are presented and compared with Adaptive Fuzzy Hierarchical Sliding Mode Control (AFHSMC) [19] as shown in figures 6-9. The position tracking plots for the pendulum and the cart (Figure 6 and 7) demonstrate the perfect match of the two control methods for a hundred seconds. As can be clearly seen for AFHTSMC, the small undesirable fluctuations disappear in the very first steps of the control algorithm and the desired oscillatory motion continues over a long period of time. Figure 8 represents a significant effect of the TSM implication on the control method by comparing the top hierarchical surfaces of the aforementioned methods. As it is shown the TSM results have a higher rate of convergence. Also, asymptotical trajectory tracking is obtained immediately and the transition time (0.42 seconds) is much less than that of [19] (3.65 seconds). In addition, the variations of the top hierarchical surface decreases significantly in AFHTSMC, compared to AFHSMC. Therefore, the combination of the TSM control and hierarchical structure enables the fast finite time convergence of the uncertain nonlinear dynamic system. Therefore, the proposed method is much more convenient when fast convergence properties and high precision are required. The control input variations after learning are also presented in figure 9, in which the AFHTSMC shows smoother force results. This happens because of the TSM requirement to avoid the singularity problem. Although there may exist a large amplitude of force before learning, it does not affect the system because of the AFHTSMC's fast convergence. However, there still exists small fluctuations. In addition, in most of the high precision applications, we do not need very large forces. Hence, the force variations are between small ranges that do not affect the system performance.

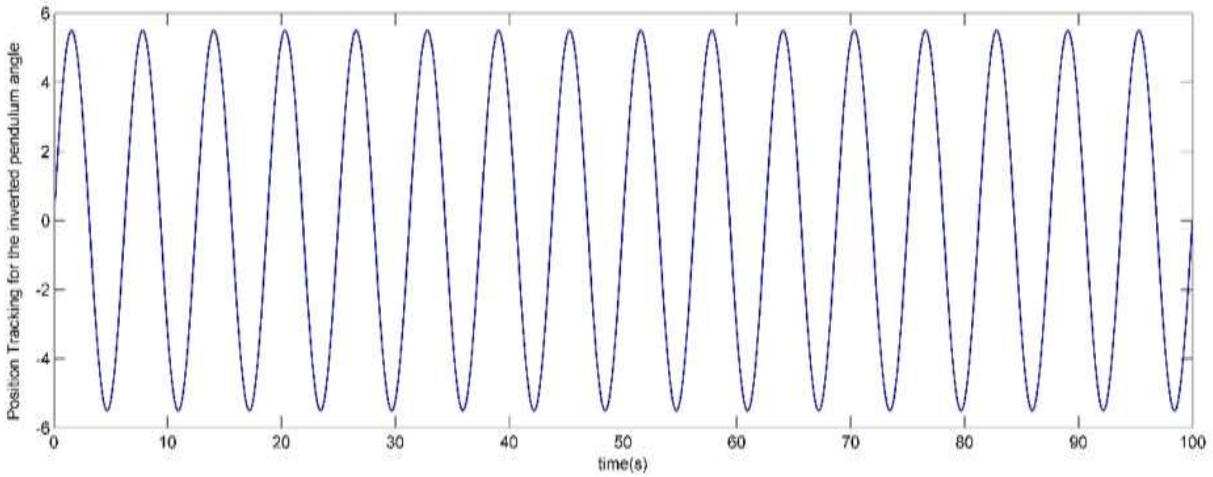

Figure 6. The position tracking vs. time for the pendulum angle (blue dashed line is the reference signal, the solid blue line is the output signal and the red dashed line is for the AFHSMC).

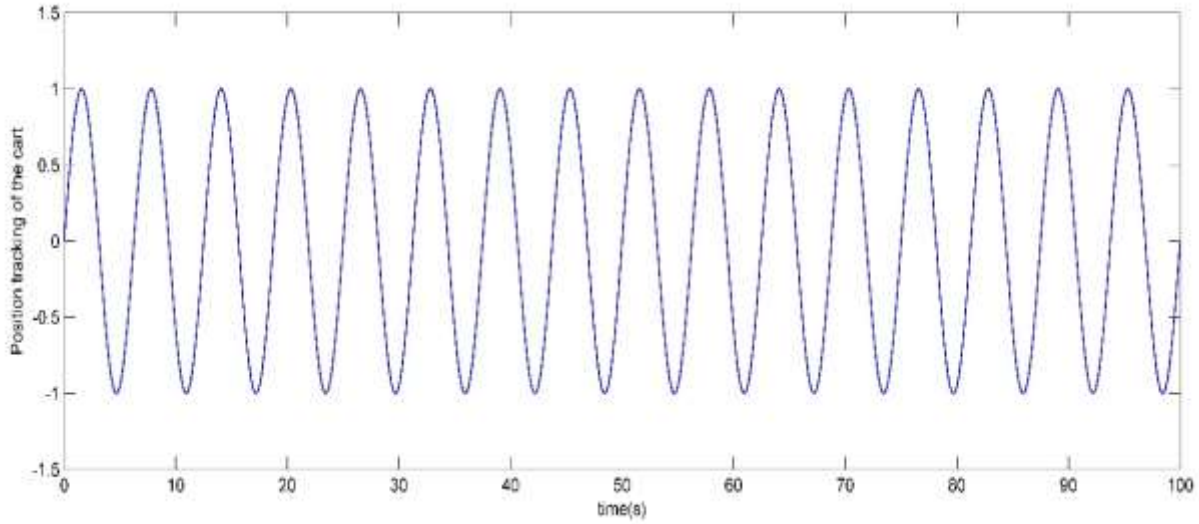

Figure 7. The position tracking vs. time for the cart (dashed blue line is the reference signal, the solid blue line is the output signal and the dashed red line is for the AFHSMC).

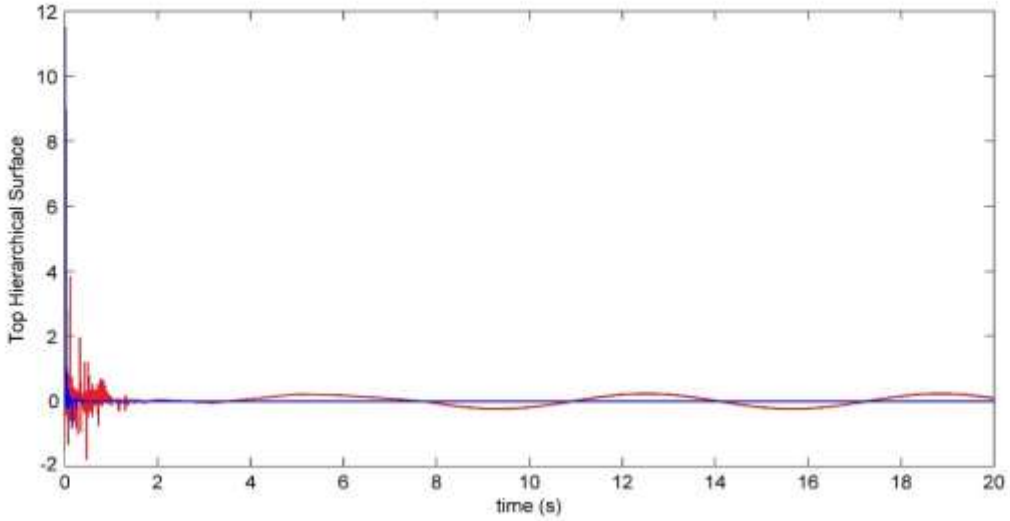

Figure 8. Second level hierarchical terminal sliding surface vs. time (blue and red solid lines represents the AFHTSMC and the AFHSMC top hierarchical surface, respectively).

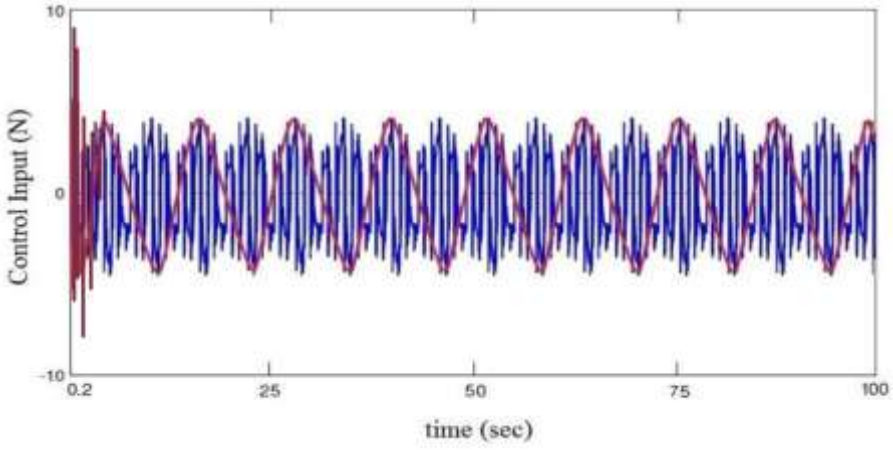

Figure 9. The control input (u) vs. time (The blue solid line and the red solid line show the force values for AFHTSMC and AFHSMC, respectively).

It is clear that larger learning rates can accelerate the convergence properties though the instability phenomena possibly occur in AFHSMC, especially in long-term applications. However, the

implementation of the AFHTSMC reduces the requirement to implement very large learning rates, and is a major drawback of the previous studies. In addition, as demonstrated in the simulation results, applying Lyapunov stability theorem with the AFHTSMC guarantees the robustness to the bounded external disturbance, stability, and finite time convergence in trajectory tracking of the system.

6. Conclusions

In this study, the AFHTSMC has been proposed for a class of uncertain nonlinear dynamic systems. The control algorithm was designed based on the Lyapunov stability criterion. The combination of the TSM and the adaptive fuzzy hierarchical system, which is the main novelty of this paper, enables the system to converge much faster to the desired trajectory compared with the other methods in literature. Also, applying the TSM in the adaptive fuzzy hierarchical system is much more effective in chattering reduction. Furthermore, the hierarchical structure decouples the class of nonlinear coupled systems to subsystems with guaranteed stability, and the direct adaptive fuzzy scheme works online but does not require prior knowledge of dynamic parameters. Computer simulations for an inverted pendulum on a cart have demonstrated the long-term stability, robustness, and validity. The AFHTSMC can be extended to other applications with multi-input-multi-output (MIMO) structures. We will focus on the fuzzy Type-2, neuro-fuzzy, and evolutionary fuzzy systems in the hierarchical TSM in our future study.

References

[1] Santiesteban, R., Floquet, T., Orlov, Y., Riachy, S. & Richard, J. P. (2008). Second Order Sliding Mode Control of Under-actuated Mechanical Systems II: Orbital Stabilization of an Inverted Pendulum with Application to Swing Up/Balancing Control, International Journal of Robust Nonlinear Control, vol. 56, no. 3, pp.529-543.

[2] Udawatta, L., Watanabe, K., & Izumi K. (2004). Control of three degrees of freedom under-actuated manipulator using fuzzy based switching, Artificial Life Robotics, vol. 8, no. 2, pp. 153- 158.

[3] Chiang, C. C., & Hu, C. C. (2012). Output tracking control for uncertain under-actuated systems based fuzzy sliding-mode control approach, IEEE International Conference on Fuzzy Systems Proceedings, Brisbane, Australia, 2012.

[4] Utkin, V. I. (1992). Sliding Modes in Control Optimization, Berlin, Heidelberg. New York: Springer-Verlag.

[5] Zinober, A. S. I. (1993). Variable Structure and Lyapunov Control, London, Heidelberg. New York: Springer-Verlag.

[6] Slotine, J. J. E. & Li, W. (1991). Applied Nonlinear Control, New Jersey: Prentice Hall.

[7] Utkin, V., Guldner, J. & Shi, J. (1999). Sliding Mode Control in Electromechanical Systems, Taylor and Francis Ltd.

[8] Yu, X.H. & Zhihong, M. (1996). Model reference adaptive control systems with terminal sliding modes, International Journal of Control, vol. 64, pp. 1165–1176.

[9] Yu, X., Zhihong, M., Feng, Y. & Guan, Z. (2002). Nonsingular terminal sliding mode control of a class of nonlinear dynamical systems, 15th Terminal world congress (IFAC), Barcelona, Spain, 2002.

[10] Zhihong, M. & Yu, X.H. (1997). Terminal sliding mode control of MIMO linear systems, IEEE Transactions on Circuits Systems: I, Fundamental Theory Applications, vol. 44, pp. 1065–1070.

[11] Wu, Y., Yu, X. & Man, Z. (1998) Terminal sliding mode control design for uncertain dynamic systems, Systems Control Letters, vol. 34, pp. 281–287.

[12] Feng, Y., Yu, X. & Man, Z. (2002). Non-singular terminal sliding mode control of rigid manipulators, Automatica, vol. 38, pp. 2159–2167.

[13] Tao, C. W., Taur, J. S. & Chan, M. L. (2004). Adaptive fuzzy terminal sliding mode controller for linear systems with mismatched time-varying uncertainties, IEEE Transactions on Systems Man and Cybernetics B. Cybernetics, vol. 34, pp. 255–262.

[14] Chiang, C. C. & Hu, C. C. (2012). Output tracking control for uncertain under-actuated systems based fuzzy sliding-mode control approach, IEEE International Conference on Fuzzy Systems Proceedings, Brisbane, Australia, 2012.

[15] Aghababa, M. P. (2014). Design of hierarchical terminal sliding mode control scheme for fractional-order systems, IET Science, Measurement & Technology, vol. 9, no. 1, pp. 122-133.

[16] Mobayen, S. (2015). Fast terminal sliding mode tracking of non-holonomic systems with exponential decay rate, IET Control Theory and Applications, vol. 9, no. 8, pp. 1294-1301.

[17] Mobayen, S. (2014), An adaptive fast terminal sliding mode control combined with global sliding mode scheme for tracking control of uncertain nonlinear third-order systems, Nonlinear Dynamics, DOI:10.1007/s11071-015-2180-4.

[18] Hwang, C. L., Wu, H. M. & Shih, C. L. (2009). Fuzzy sliding-Mode under-actuated control for autonomous dynamic balance of an electrical bicycle, IEEE Transactions on Control Systems and Technology, vol. 17, no. 3, pp. 783–795.

[19] Nekoukar, V. & Erfanian, A. (2011). Adaptive fuzzy terminal sliding mode control for a class of MIMO uncertain nonlinear systems, Fuzzy sets and systems, vol. 179, pp. 34-49.

[20] Lin, C. M. & Mon, Y. J. (2005). Decoupling control by hierarchical fuzzy sliding-mode controller, IEEE Transactions on Control Systems and Technology, vol. 13, no.4, pp. 593–598.

[21] Qian, D., Yi, J. & Zhao, D. (2008). Control of a class of under-actuated systems with saturation sing hierarchical sliding mode, IEEE International Conference on Robotics and Automation Proceedings, Pasadena, CA, USA, 2008.

[22] Hwang, C. L., Chiang, C. C. & Yeh, Y. (2014). Adaptive Fuzzy Hierarchical Sliding-Mode Control for the Trajectory Tracking of Uncertain Under-actuated Nonlinear Dynamic Systems, IEEE Transactions on Fuzzy Systems, vol. 22, no. 2, pp. 286-299.

[23] Li, T. & Huang, Y., (2010). MIMO adaptive fuzzy terminal sliding-mode controller for robotic manipulators, Information Siences, vol. 180, pp. 4641-4660.

نشریه هوش مصنوعی و داده‌کاوی

تعقیب مسیر ربات‌های دینامیکی غیرخطی زیرفعال: کنترل مد لغزشی ترمینال سلسله‌مراتبی فازی تطبیقی

یاسمن واقعی و انوشیروان فرشیدیانفر*

[1]گروه مهندسی مکانیک، دانشگاه فردوسی مشهد، مشهد، ایران.

ارسال ۲۰۱۵/۰۴/۲۱ ؛ پذیرش ۲۰۱۵/۱۱/۲۸

چکیده:

در سال‌های اخیر، تعقیب مسیر در سیستم‌های دینامیکی غیرخطی زیرفعال مانند روبات‌های فضایی و عملگرهای انعطاف‌پذیر به‌دلیل نیاز به محاسبات پیچیده توسط کنترل مد لغزشی سلسله مراتبی مورد بررسی قرار گرفته است. با این حال، امکان به‌وقوع پیوستن پدیده‌ی ناپایداری به‌خصوص در کاربری‌های طولانی‌مدت وجود دارد. در این پژوهش، روش طراحی نوینی از کنترل‌کننده‌ی مد لغزشی ترمینال سلسله مراتبی فازی تطبیقی ارائه شده است. سطوح لایه‌های لغزشی زیرسیستم‌ها، ساختار سلسله مراتبی روش حاضر را تشکیل می‌دهند که در آن، لایه‌ی بالایی تمامی سطوح لغزشی زیرسیستم‌ها را شامل می‌شود. همچنین، از مود لغزشی ترمینال در هر لایه جهت اطمینان از همگرایی پاسخ به صفر در زمان محدود و نیز برای کاهش اغتشاشات استفاده شده است. به‌علاوه، مدل‌های فازی برخط نیز برای تقریب زدن دو تابع دینامیکی غیرخطی سیستم به‌کار گرفته شده‌اند. درنهایت، مثالی شبیه‌سازی شده از یک آونگ معکوس به‌منظور اثبات کارآیی و مقاومت کنترل‌کننده‌ی ارائه شده آورده شده است.

کلمات کلیدی: سیستم فازی تطبیقی، ساختار سلسله مراتبی، کنترل مد لغزشی ترمینال، سیستم‌های زیر فعال.